

Optical and AFM analysis of defect induced in lithium fluoride by energetic lead ions

H.Benhacine^{1*}, A.Meftah¹, M.Izerrouken², S.Kadid¹

¹LRPCSI, Université 20 août 55 Skikda, Route El-Hadaeik, Skikda, (ALGERIA)

²Centre de Recherche Nucléaire de Draria, BP 43, Sebbala, Draria, Algiers, (ALGERIA)

E-mail : hbenhacine@gmail.com

ABSTRACT

Single crystal samples of lithium fluoride irradiated at normal incidence with swift heavy ion Pb^{+52} of energy between 140 and 840 MeV in the fluence range 1×10^9 - 4×10^{12} ions/cm² are characterized by optical measurements (absorption and photoluminescence) and Atomic Force Microscopy (AFM). Optical measurements show that F center concentration increases with increasing fluence and reaches saturation at higher fluences.

On the other hand, F center aggregates F_2 and F_3^+ increase linearly in the same fluence range. The track radius deduced, using a model of saturated track, increases linearly with electronic stopping power. It extends from 9 to 22 nm when mean energy loss respectively varies from 11 to 25 eV/nm. The ion induced damage on the surface is observed by AFM under ambient conditions. AFM reveals circular damage zones, consisting of small hillocks. The mean diameter of the track cross sections depends on electronic stopping power $(dE/dx)_e$ and varies from 9 to 16 nm and with heights of a few nanometers. © 2014 Trade Science Inc. - INDIA

KEYWORDS

Swift heavy ions;
Optical absorption;
PL;
AFM.

INTRODUCTION

The formation of defects in lithium fluoride and in other alkali halides created under various types of irradiation, e.g. neutrons^[1], photons^[2], electrons^[3-5], and ions^[6-13] has been studied for a long time by several groups. These materials are useful in many applications like radiation dosimetry, detectors for ionizing radiations and tunable color center lasers, optical isolators in high-power laser amplifiers, generation of ultra-short pulses, and generation of difference frequencies in the infra red (IR) ranges. The optical properties of this ma-

terial can be modified by point and extended defects, created due to different types of particle irradiation. The defect centers induced by ion irradiation in LiF are mainly F center, and more complex defects F-aggregate centers such as F_2 , F_3 and F_4 .

Schwartz et al^[14] reported that single defects such as F and F_2 centers are produced in a large halo with a radius of several tens of nanometers around the ion trajectory. Above a critical energy loss of about 10 keV/nm, new effects occur within a very small core region of about 2–4 nm in diameter. They concluded that in this core region, the defects are complex aggregates such as

Full Paper

small Li colloids, and fluorine and vacancy clusters. The ion-induced damage on the surface inspected by scanning force microscopy is reported by Müller et al^[15-17]. SFM reveals circular damage zones consisting of small hillocks. The mean diameter of the track cross sections depends linearly on the ion-energy loss.

Despite such numerous published papers, only few experimental studies of F center aggregates (F_2^+ and F_3^+) induced in LiF crystal by ion irradiation are available. In the present work, in addition to the well-known F-center evolution as a function of fluence and electronic stopping power, F_3^+ , and F_3^+/F_2^+ ratio are investigated using photoluminescence spectroscopy. Atomic Force Microscopy is the complementary technique used to study the morphology of the surface after irradiation.

EXPERIMENTAL PROCEDURE

LiF samples with a varying thickness, between 0.5 and 1 mm, were cleaved along the (100) plane from a single crystal block of high purity. The crystals of LiF have been irradiated at room temperature under normal incidence with ^{208}Pb ions of 900 MeV energy delivered by the Medium Energy Line of the GANIL (Caen, France). The fluence extended from 10^8 to 4×10^{12} ions/cm² and the flux was about 4×10^8 ions cm⁻² s⁻¹ on a 1 cm² surface. Thin aluminum foils of different thicknesses were placed in front of each sample in order to modify the initial energy of the ions and consequently the range R , and electronic energy loss S_e . The range was in most cases less than the thickness of the crystals, such that the ions were stopped in the crystals. The main irradiation parameters are deduced from TRIM

TABLE 1: Irradiation parameters of Pb ions in LiF crystals. The mean electronic energy loss $\langle S_e \rangle$ is calculated from initial beam energy E divided by the range R

Energy (MeV) $^{208}\text{Pb}^{+53}$	S_e (keV/nm)	Range R (μm)	$\langle S_e \rangle =$ E/R (keV/nm)	Fluence (ϕ) Ions/cm ²
840	27	40	18	$10^8 - 4 \times 10^{12}$
544	27.5	29	16.5	$10^8 - 4 \times 10^{12}$
255	25	18	13	$10^{10} - 4 \times 10^{12}$
144	20	13	10	$10^{10} - 4 \times 10^{12}$

2003^[18] code calculations which are listed in TABLE 1.

After irradiation, the optical absorption measurements and the photoluminescence were carried out using Lambda Perkin Elmer spectrometer and Perkin-Elmer LS50B Luminescence Spectrometer. The concentration of defects is determined by the Smakula formula, modified by Dexter^[19,20]:

$$N(\text{cm}^{-3}) = A \cdot \frac{n}{(n^2 + 2)^2} \cdot \frac{W(\text{eV})}{f} \alpha_{\text{max}}(\text{cm}^{-1}) \quad (1)$$

Where f is the oscillator strength of the optical transition, n the refractive index, α_{max} the absorption coefficient measured at the maximum of the band peak and W the band's full-width at half maximum (FWHM). A is a constant, equal to $0.87 \times 10^{17} \text{ eV}^{-1} \text{ cm}^{-2}$ for Gaussian bands. The absorption coefficient α_{max} was determined from the optical spectra of each sample using the relation: $\alpha_{\text{max}} = 2.304 \text{ OD}/R$ where $\text{OD} = \log_{10}(I_0/I)$ represents the optical density at band maximum and R is the ion range.

The surface topography of the irradiated samples was analyzed using AFM. The measurements were performed, under ambient conditions, operating in the tapping mode at a cantilever resonance frequency of 75 kHz, and the oscillation amplitude of 3V. The AFM images were recorded by reflecting a laser beam from the backside of the force sensing cantilever and monitoring its displacements on a four-quadrant photodiode.

RESULTS AND DISCUSSION

Optical measurements

Optical absorption and photoluminescence measurements are made in the range 190 – 900 nm and 450 (2.75) – 800 nm (1.55 eV), respectively. All measurements are made at room temperature.

Optical absorption measurements

Typical optical absorption spectra obtained with LiF crystals irradiated with 840 MeV Pb ions at different fluence values ranging from 10^{11} to 4×10^{12} ions/cm² are reported in Figure 1. The spectra show two predominant absorption bands around 245 and 445 nm. The absorption band 245 is attributed to F-center (one electron trapped in one anion vacancy) and the 445 nm band is the contribution of respectively F_2^- -centers (445

nm) (two electrons trapped in two neighboring anion vacancies) and F_3^+ - centers (458 nm) (two electrons trapped in three neighboring anion vacancies). At higher fluences ($\phi > 2 \times 10^{11}$ ions/cm²) the spectra become more complex and shoulders at about 315, 375, 515 and 545 nm are observed. All these bands are well known, 315 and 375 nm are attributed to F_3 -center (three electrons trapped in three neighboring anion vacancies) and 515 and 545 nm are due to F_4 -center (four electrons trapped in four neighboring anion vacancies).

The F-center concentration N_F calculated using Eq. 1 is presented as a function of fluence in Figure 2 for Pb ions with different specific energies 4.1, 2.6, 1.2, 0.7 MeV/u. At lower fluence, N_F follows a linear increase. Above 4×10^{11} ions/cm², N_F saturates reaching a maximum value of 1×10^{19} .cm⁻³ when the entire crystal surface is covered by tracks.

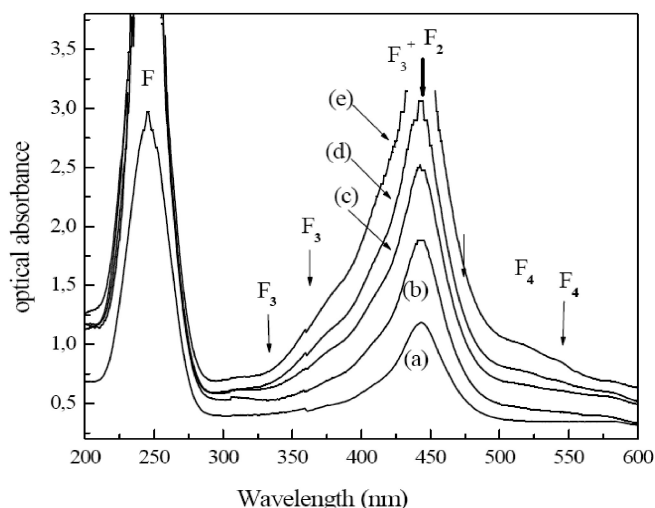


Figure 1 : Optical absorption spectra of LiF crystals irradiated with Pb ions (4.1 MeV/u) of various fluences: (a) 1×10^{11} cm⁻², (b) 2×10^{11} cm⁻², (c) 4×10^{11} cm⁻², (d) 8×10^{11} cm⁻² and (e) 4×10^{12} cm⁻². The absorbance of F and F_2 centres increases with ion fluence

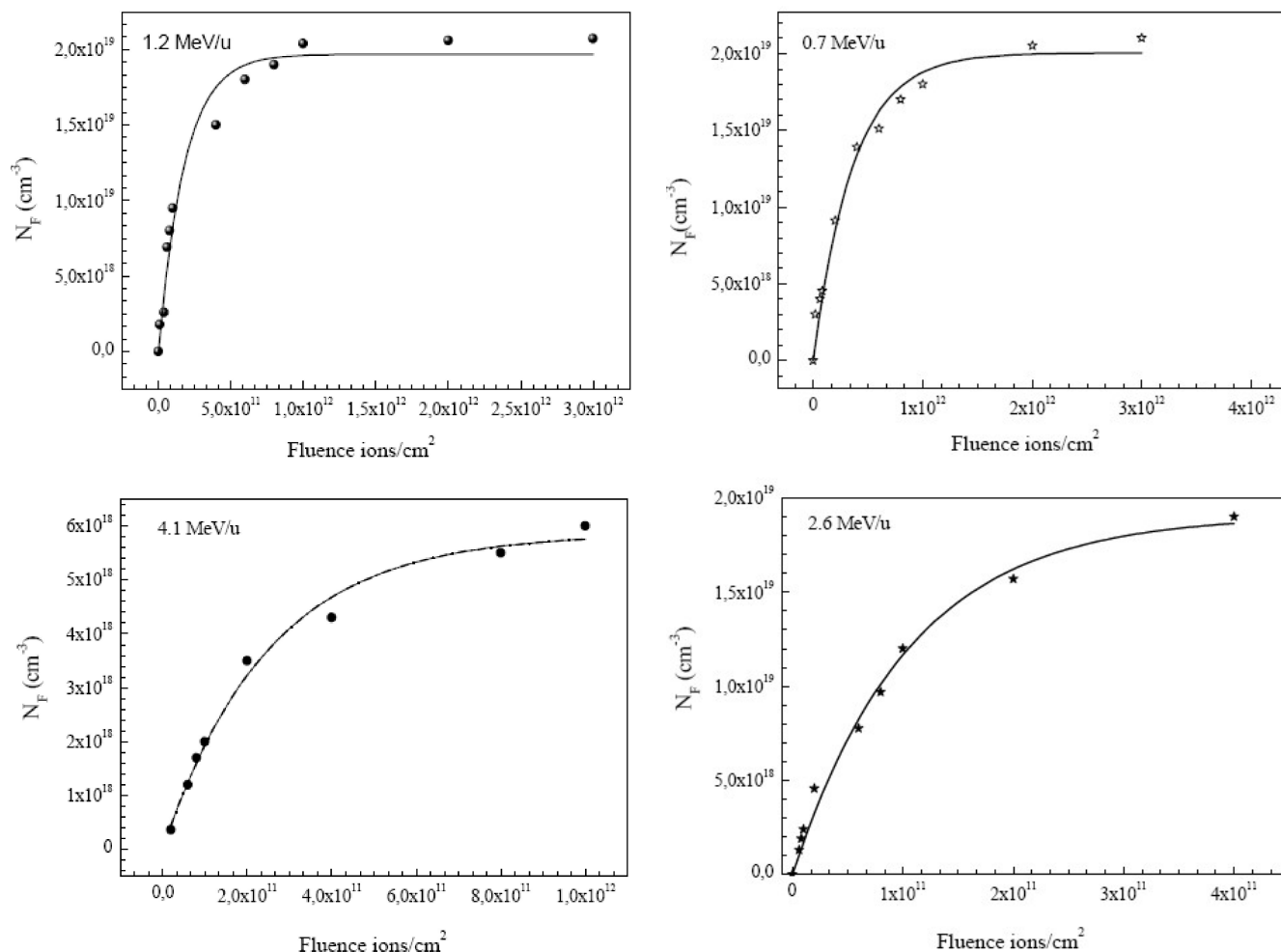


Figure 2 : Concentration of F-centers as a function of the fluence of Pb ions with different specific energies 4.1, 2.6, 1.2, 0.7 MeV/u. The concentration of F centers increases exponentially with ion fluence and saturates at higher fluences

Full Paper

Approximately the same value was observed by Trautmann et al.^[11] and is attributed to the overlapping of neighboring tracks.

Using the simple model proposed by Thévenard et al.^[1], assuming that F-centers are homogeneously distributed in a cylindrical volume around the ion trajectory, the F-center creation obtained from this model is in the form:

$$N_F = N_s (1 - \exp(-\pi r^2 \Phi)) \quad (2)$$

Where N_s (cm^{-3}) is the saturated concentration of F-centers in each individual track, and r is the track radius. From the fit of the experimental data using Eq.2, the track radius is deduced and presented in Figure 3 as a function of mean energy loss. The track radius r , fits of such saturation curves give a value between 9 nm for 0.7 MeV/u and almost 22 nm for energy 4.1 MeV/u. The data show the track radius increases with increasing mean energy loss.

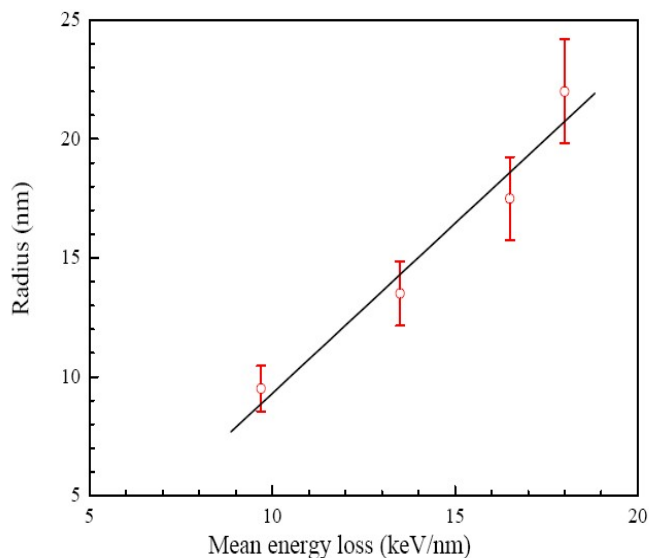
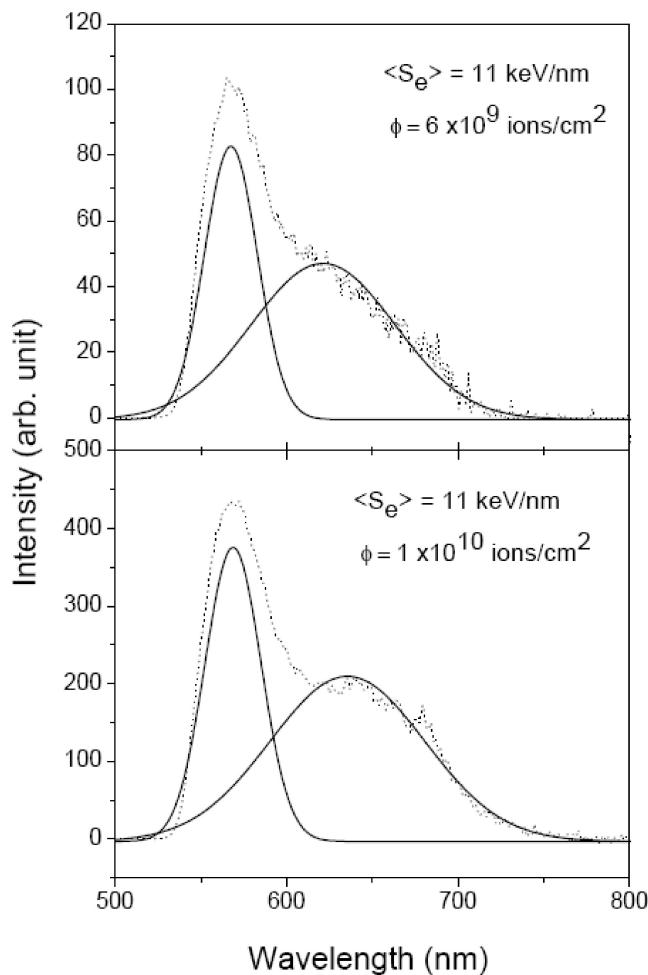
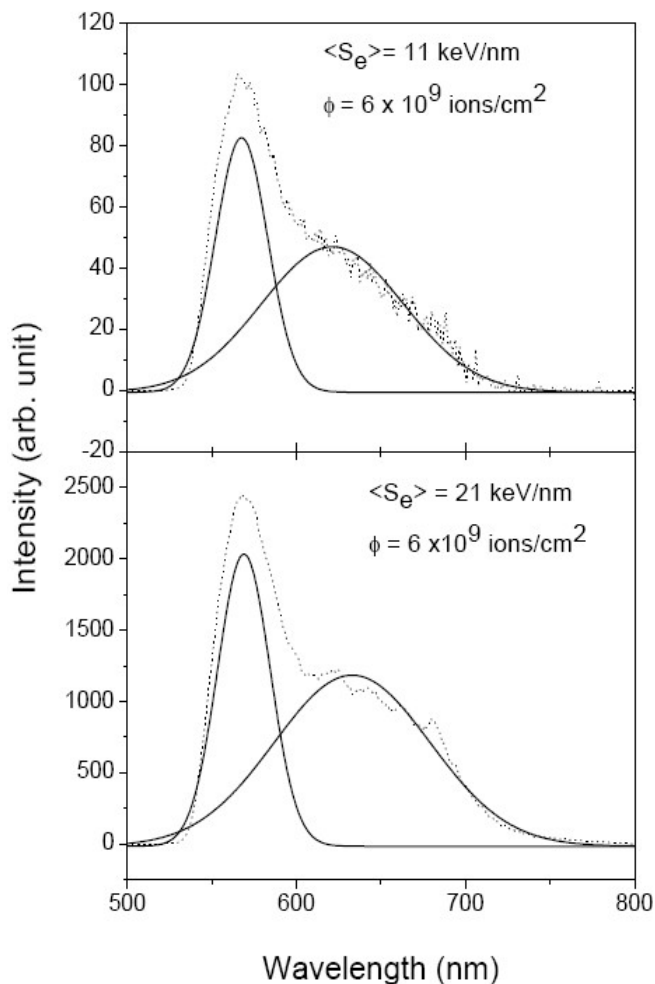


Figure 3 : Track radii in LiF deduced from optical absorption bands of F-centers plotted versus the mean energy loss



(a)



(b)

Figure 4 : Photoluminescence spectra of LiF crystals (a) irradiated with 144 MeV Pb ions at different fluence, (b) irradiated with Pb ions of different electronic stopping power

Photoluminescence measurements

The photoluminescence technique allows the possibility to study with more precision the F_3^+ and F_2 centers. The emission bands of F_3^+ and F_2 centers are well resolved contrary to their absorption bands. The excitation with a 445 nm wavelength-photon induces emission bands centred at about 553 nm and 680 nm assigned to F_3^+ and F_2 centers respectively^[21,22]. Moreover, The linear dependence between luminescence intensity and the number of related radiation defects is

only valid at significantly lower values of optical density (<0.4). Thus only F_2 and F_3^+ with optical density lower than 0.5 is considered. Figure 4 shows an example of photoluminescence spectra of LiF single crystal irradiated with Pb ions at different fluence and electronic stopping power. As mentioned above the spectra show two emission bands with maxima at about 2.17 eV (570 nm) and 1.95 eV (640 nm) due to the luminescence of F_3^+ and F_2 centers^[23,24] respectively. The solid line in the figures is the fit of the experimental data using two

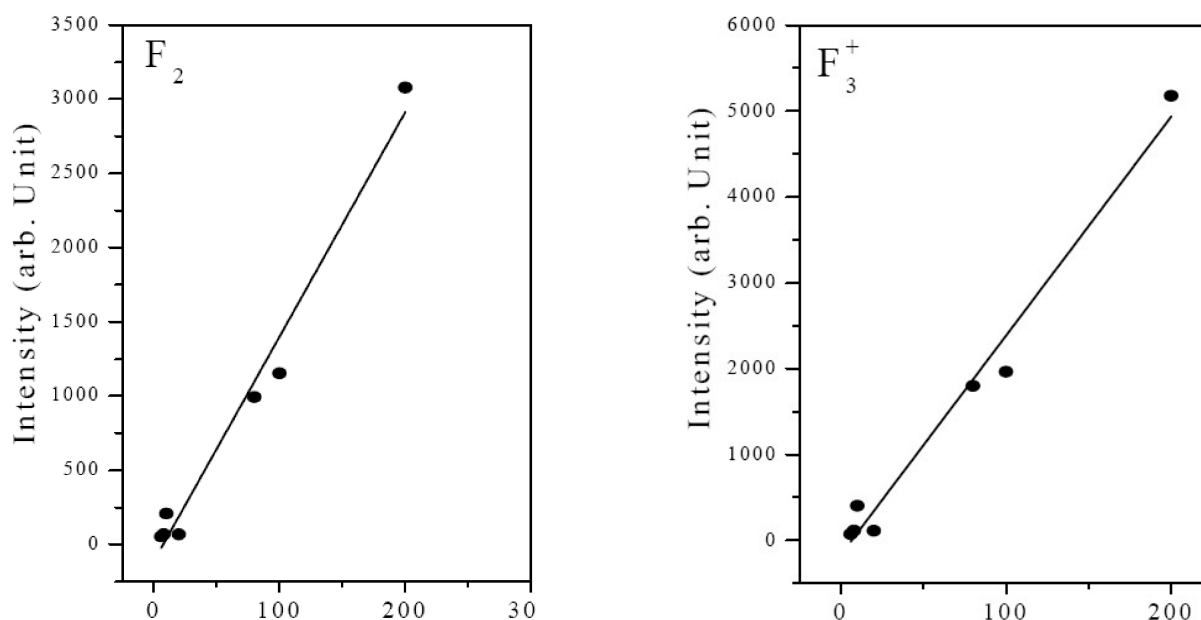


Figure 5 : PL intensity F_2 and F_3^+ color centers as a function of fluence

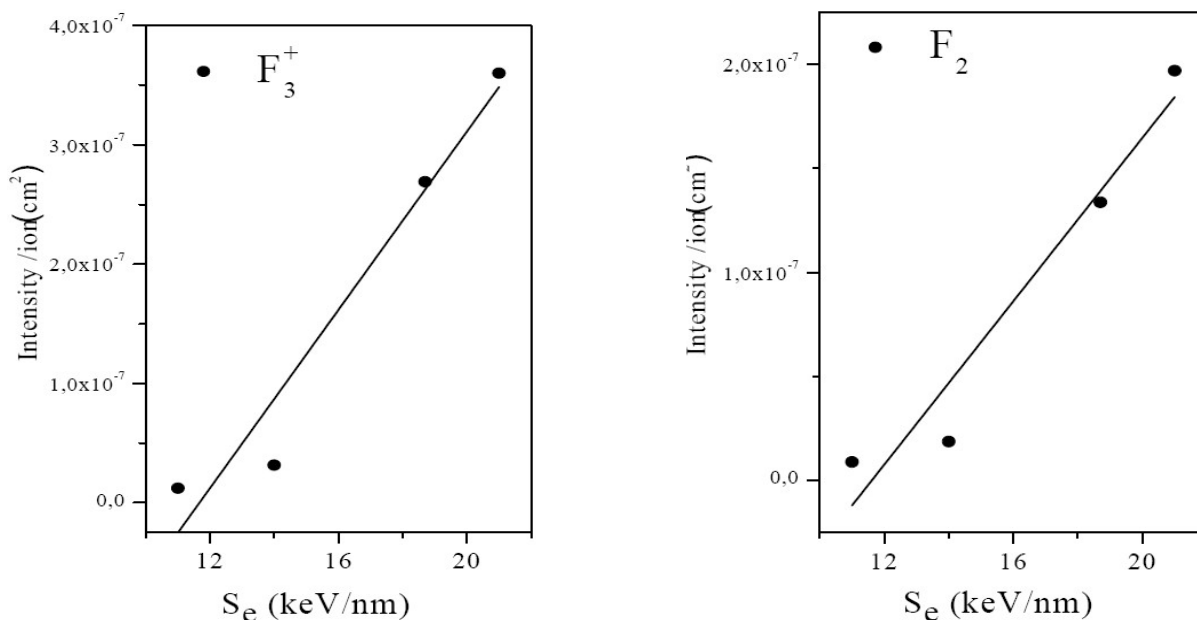


Figure 6 : PL intensity F_2 and F_3^+ color centers as a function of mean energy loss

Full Paper

Gaussian peaks.

The fit reveals approximately the same emission band width with increasing fluence and electronic stopping power. The F_2 and F_3^+ intensities linearly increase with increasing fluence as shown in Figure 5.

An approximately linear relationship is also observed between the intensities and the mean energy loss (see Figure 6).

According to our experimental data illustrated in the Figure 7, it is clear that the concentration ratio between F_3^+ and F_2 centers (F_3^+/F_2) increase with increasing fluence and electronic stopping power. This indicates the dependence of F_3^+/F_2 ratio on irradiation parameters as already expected by Baldachini et al.^[25]. At high fluence ($> 10 \times 10^9$ ion/cm²) and higher electronic stopping power (> 18 keV/nm) the ratio F_3^+/F_2

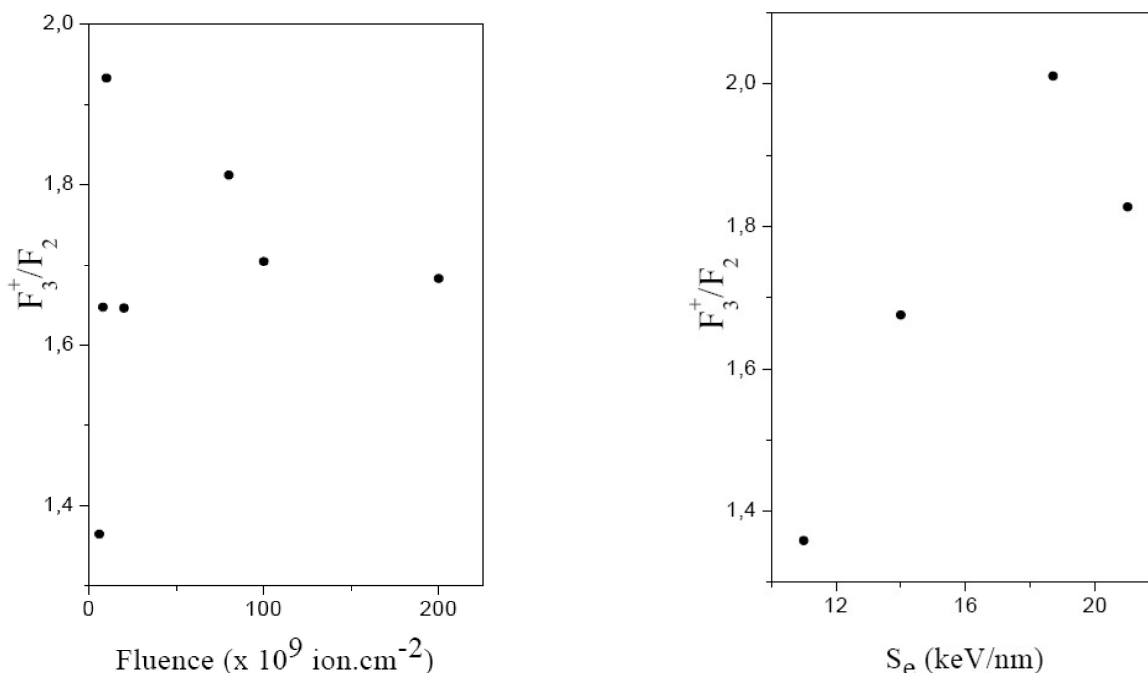


Figure 7 : The variation of the intensity ratio between F_3^+ and F_2 color centers with fluence and electronic stopping power

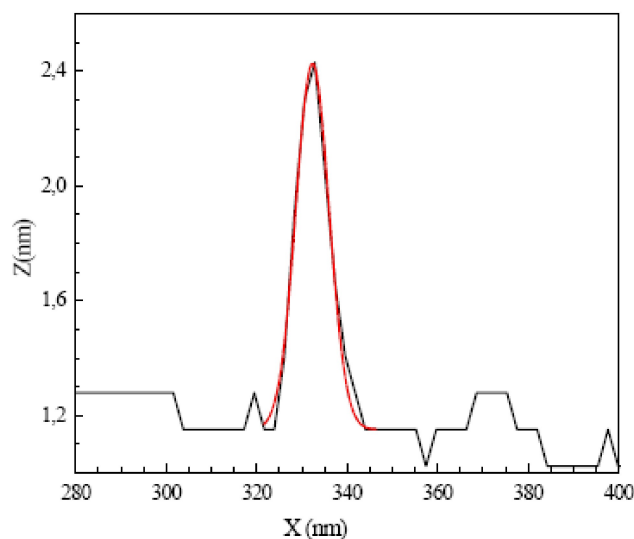
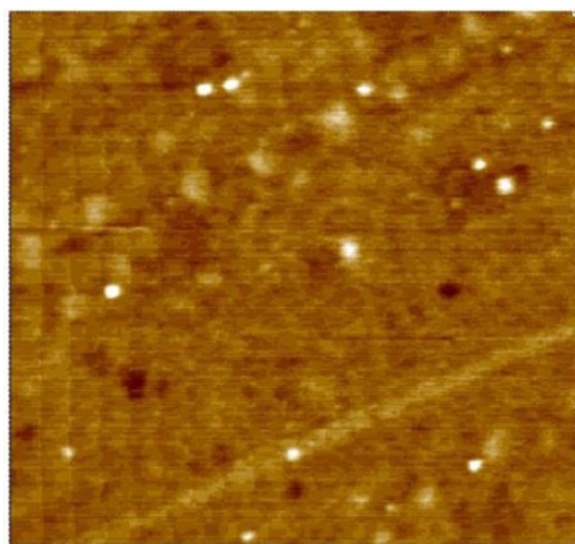


Figure 8 : Topographic AFM image (500×500 nm²) of a LiF surface irradiation with 4.1 MeV/u Pb^{53+} ions at fluence of 4×10^9 cm⁻². The light impact zones of the ions are hillocks. The line structures correspond to surface steps originating from the cleaving process. The figure on the right presents a line scan over one of the hillocks.

reaches a constant value of about 1.8. Thus at higher fluence, the F_3^+ luminescence intensity is approximately twice the F_2 intensity in accordance with the Kumar et al.^[26] findings in the case of nano-granular LiF thin film.

Atomic force microscopy

Topographic image of LiF sample irradiated with 4.1 MeV/u Pb ions at a fluence of 4×10^9 ions/cm² and the corresponding cross-sectional profile are presented in Figure 8. The light dot in the image corresponds to the hillocks induced by ions impact.

Each individual hillock was fitted by Gaussian to determine the height and diameter at FWHM. About forty hillocks was analyzed for each sample and presented like a histogram in Figure 9.

The mean height and diameter extracted from such distribution for Pb ions with different electronic stopping power S_e are summarized in TABLE 2. The mean diameter and height of the tracks increases with electronic energy loss. Similar evolution were also observed in the case of others materials such as LaF₃^[27], CaF₂^[28-30], and LiNbO₃^[31].

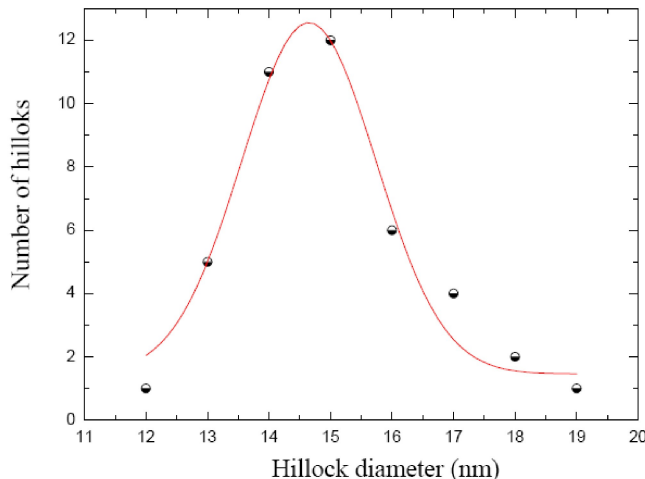


Figure 9 : Histogram of hillock diameter induced by 4.1 MeV/u Pb ions at fluence of 4.10^9 cm⁻²

TABLE 2 : The hillocks height and diameter for LiF crystal irradiated with 544 and 840 MeV Pb ions measured from AFM.

Energy (MeV)	S_e (keV/nm)	Ion fluence (cm ⁻²)	Height (nm)	Diametre (nm)
840	27	4×10^9	1.4 ± 0.2	10 ± 1
544	27.5	4×10^{10}	1.9 ± 0.4	13.5 ± 1.5

CONCLUSIONS

This paper reports on the damage produced in LiF single crystals by irradiation with lead ions at different energies and fluences. In the initial stage of irradiation, the F-center creation increases linearly and saturates at higher fluences. Single defects such as F-centers are produced in a large halo of 9–22 nm around the ion trajectory and track radii increases with the mean energy loss. Photoluminescence spectroscopy reveals that F centers aggregates (F_3^+ , F_2) increase linearly with increasing fluence and electronic energy loss, where as the F_3^+/F_2 ratio reaches saturation value of about 1.8. According to our experimental data at higher fluence F_3^+ intensity is twice the F_2 center concentration. Furthermore, the surface defect investigated by AFM technique reveals that hillocks parameter (Height, diameter) increase as a function of electronic energy loss.

ACKNOWLEDGEMENTS

The authors are particularly indebted to Dr. M. Toulemonde to have placed at our disposal the single crystals of LiF used in this study within the framework of project CMEP, Tassil 03, MDU 573, and Dr. L. Gerbous from Nuclear Research Center of Algiers for photoluminescence measurements.

REFERENCES

- [1] P.Thevenard, G.Guiraud, C.H.S.Dupuy, B.Delaunay; Radiat.Eff., **32**, 83 (1977).
- [2] G.Baldacchini, F.Bonfigli, A.Faenov, F.Flora, R.M.Monteriali, D.Murra, E.Nichelatti, T.Pikuz; Radiat.Eff.DefectsSolids, **157**, 69 (2002).
- [3] W.Gellermann, A.Müller, D.Wandt, S.Wilk, F.Luty; J.Appl.Phys., **61**, 1297 (1987).
- [4] G.Baldacchini, F.Bonfigli, F.Menchini, R.M.Monteriali; Nucl.Instr.and Meth.B, **191**, 216 (2002).
- [5] R.M.Monteriali; Radiat.Eff.Defects Solids, **157**, 545 (2002).
- [6] K.Schwartz, G.Wirth, C.Trautmann, T.Steckenreiter; Phys.Rev.B, **56**, 10711 (1997).
- [7] C.Trautmann, K.Schwartz, J.M.Costantini, T.Steckenreiter, M.Toulemonde; Nucl.Instr.and Meth.B, **146**, 367 (1998).

Full Paper

- [8] V.A.Skuratov, S.M.Abu AlAzm, V.A.Altynov; Nucl.Instr.And Meth.B, **191**, 251 (2002).
- [9] M.Kumar, F.Singh, S.A.Khan, V.Baranwal, S.Kumar, D.C.Agarwal, A.M.Siddiqui, A.Tripathi, A.Gupta, D.K.Avasthi, A.C.Pandey; J.Phys.D:Appl. Phys., **38**, 637 (2005).
- [10] C.Trautmann, K.Schwartz, O.Geiß; J.Appl.Phys., **83**, 3560 (1998).
- [11] C.Trautmann, M.Toulemonde, K.Schwartz, J.M.Costantini and A.Müller; Nucl.Instr.And Meth B, **164**, 365 (2000).
- [12] E.Balanzat, S.Bouffard, A.Cassimi, E.Dooryhee, L.Protin, J.P.Grandin, J.L.Doualan, J.Margerie; Nucl.Instr.and Meth B, **91**, 134 (1994).
- [13] A.T.Davidson, K.Schwartz, J.D.Comins, E.G.Kozakiewicz, M.Toulemonde, C.Trautmann; Phys.Rev.B, **66**, 214102 (2002).
- [14] K.Schwartz, C.Trautmann, T.Steckenreiter, O.Geiß, M.Krämer; Phys.Rev.B, **58**, 11232 (1998).
- [15] A.Müller, R.Neumann, K.Schwartz, C.Trautmann; Nucl.Instr.and Meth B, **146**, 393 (1998).
- [16] Müller, C.Müller, R.Neumann, F.Ohnesorge; Nucl.Instr.and Meth B, **166**, 581 (2000).
- [17] Müller, M.Cranney, A.S.El-Said, N.Ishikawa, A.Iwase, M.Lang, R.Neumann; Nucl.Instr.and Meth.B, **191**, 246 (2002).
- [18] J.F.Ziegler, P.Biersack, U.Littmark, J.F.Ziegler; Pergamon, New York, (1985).
- [19] A.Smakula; Z.Physik, **59**, 603 (1930).
- [20] L.Dexter; Phys.Rev., **48**, 101 (1956).
- [21] V.A.Skuratov, S.M.Abu AlAzm, V.A.Altynov; Nuc.Instr.AndMeth, **B191**, 251 (2002).
- [22] G.Baldacchini, R.M.Montereali; Opt.Mater., **16**, 53 (2001).
- [23] F.Bonfigli, B.Jacquier, R.M.Montereali, P.Moretti, V.Mussi, E.Nichelatti, F.Somma; Opt.Mater., **24**, 291 (2003).
- [24] K.Kawamura, M.Hirano, T.Kurobori, D.Takamizu, T.Kamiya; H.Hosono.Appl.Phys.Lett., **84**, 311 (2004).
- [25] G.Baldacchini, E.De Nicola, G.Giubileo, F.Menchini, G.Messina, R.M.Montereali, A.Scacco; Nucl.Instr. and Meth.B, **141**, 542 (1998).
- [26] M.Kumar, F.Singh, S.A.Khan, A.Tripathi, D.K.Avasthi, A.C.Pandey; J.Lum., **127**, 302 (2007).
- [27] A.S.El-Said, R.Neumann, K.Schwartz, C.Trautmann; Surface and Coatings Technology, **158**, 522 (2002).
- [28] N.Khalfaoui, C.C.Rotaru, S.Bouffard, M.Toulemonde, J.P.Stoquert, F.Haas, C.Trautmann, J.Jensen, A.Dunlop; Nucl.Instr.andMeth.B, **240**, 819 (2005).
- [29] A.S.El-Said, W.Meissl, M.C.Simon, J.R.Crespo López-Urrutia, I.C.Gebeshuber, M.Lang, H.P.Winter, J.Ullrich, F.Aumayr; Nucl.Instr.and Meth, **B256**, 346 (2007).
- [30] Müller K.-O.Voss, M.Lang, R.Neumann; Nucl. Instr.and Meth.B, **212**, 729 (2003).
- [31] B.Canut, S.M.M.Ramos, R.Brenier, P.Thévenard, J.L.Loubet, M.Toulemonde; Nucl.Instr. and Meth.B, **107**, 194 (1996).